

Chapter 18

Amplification of Radiation in a Doped Glass Fiber

We study the dynamics of gain of fiber amplifiers and fiber lasers. We present a model—the quasiband model—that allows for derivation of an analytical expression for the gain coefficient of an optically pumped doped glass fiber. We concentrate the discussion mainly on the erbium-doped fiber amplifier. We will however discuss other fiber amplifiers and fiber lasers too.

A glass fiber of the worldwide optical fiber network contains, about every 50 km, an erbium-doped fiber amplifier. This amplifier operates in a frequency band (width ~ 5 THz) around 195 THz ($1.54 \mu\text{m}$). It is possible to pump the erbium-doped fiber amplifier with radiation of a semiconductor laser at a frequency (~ 202 THz) that lies just outside the range of gain. Alternatively, pumping with radiation at a much larger frequency is possible.

While an excited atom in a gas, a liquid, or a crystal keeps its excitation until a stimulated emission process takes place, the situation is completely different for a fiber glass medium. In a glass, an excited ion loses its excitation to another ion and this to a third ion and so on—the excitation migrates within the glass. The origin of the migration of excitation are phonon-assisted energy transfer processes. An excitation travels over a very large number of ions before a stimulated emission process takes place. The migration of excitation plays an essential role in the dynamics of gain of radiation in fiber amplifiers. We will introduce a model (quasiband model) that takes account of the migration of energy and that enables us to calculate the gain coefficient of a fiber.

We will begin this chapter with a short survey of the erbium-doped fiber amplifier: we first describe the gain coefficient and the quasiband model. Later in the chapter, we will justify the model and derive the gain coefficient. In the last section of the chapter, we will show that the quasiband model is in accord with experimental results of absorption, fluorescence, and gain measurements. We will also discuss three-level laser models often used for description of fiber lasers and amplifiers.

18.1 Survey of the Erbium-Doped Fiber Amplifier

Figure 18.1 shows the gain coefficient of an *erbium-doped fiber amplifier*; the gain coefficient was calculated (Sect. 18.6) under the assumption that $\sim 60\%$ of the erbium ions are in the excited state. The amplifier operates in a wavelength range near $1.54 \mu\text{m}$ (frequency 195 THz); *see* also Table 18.1. The gain bandwidth of about 40 nm ($\sim 5 \text{ THz}$) corresponds to $\sim 2.5\%$ of the center frequency. Radiation of a semiconductor laser serves as pump laser (pump wavelength $1.48 \mu\text{m}$, frequency $\sim 203 \text{ THz}$). According to the small difference between pump and laser wavelength, it is possible to reach a high quantum efficiency of conversion of pump radiation to laser radiation. The model of a glass fiber amplifier, presented in this chapter, has been published in 2010 [145].

We begin with mentioning few data of an erbium-doped fiber amplifier:

- Density of SiO_2 glass = $2.3 \times 10^3 \text{ kg m}^{-3}$, corresponding to an SiO_2 number density of $2.3 \times 10^{28} \text{ m}^{-3}$.
- $N_0 = 7 \times 10^{25} \text{ m}^{-3}$ = density of Er^{3+} ions, corresponding to one Er^{3+} ion per 330 SiO_2 units; molar concentration of Er_2O_3 in quartz glass = 1,500 ppm = 1% by weight Er_2O_3 in SiO_2 glass.
- N = density of excited Er^{3+} ions.
- $\Delta\nu_g = 5 \text{ THz}$ = gain bandwidth.
- Wavelength of maximum gain; $\lambda = 1.54 \mu\text{m}$ (frequency 195 THz).
- Refractive index of quartz glass; $n = 1.5$.

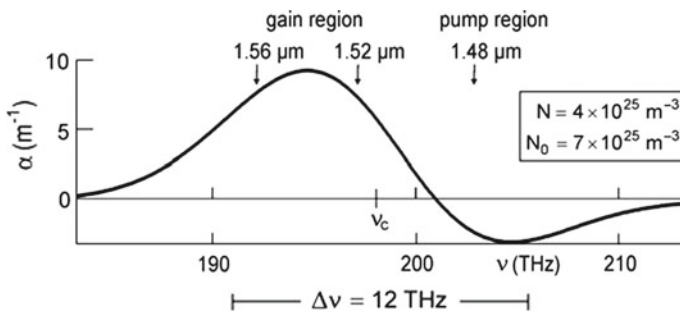
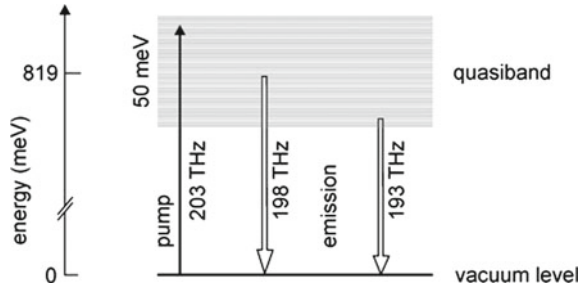


Fig. 18.1 Gain coefficient of an erbium-doped fiber

Table 18.1 Erbium-doped fiber amplifier

	λ	ν (THz)	Energy (meV)
Gain region	1.52–1.56 μm	193–197	799–815
Center of gain region	1.54 μm	195	807
Gain bandwidth	40 nm	5	20
Pump	1.48 μm	203	840

Fig. 18.2 Principle of the erbium-doped fiber amplifier



- $\tau_{\text{sp}} \sim 10 \text{ ms}$ = spontaneous lifetime of the upper laser levels.
- $\alpha = 9 \text{ m}^{-1}$ = maximum gain coefficient at a density of excited Er^{3+} ions of $N = 4 \times 10^{25} \text{ m}^{-3}$.
- Effective gain cross section at the wavelength of maximum gain $\sigma_{21} = 3 \times 10^{-25} \text{ m}^2$; *see* Sect. 18.7.
- Gain factor for a fiber of 10 m in length $G = 3 \times 10^3$; this correspond to a gain of 3.5 dB m^{-1} .
- Pump rate

$$r = N/\tau_{\text{sp}} \sim 4 \times 10^{27} \text{ m}^{-3} \text{ s}^{-1}; \quad (18.1)$$

this corresponds to a pump power $P = r \times V \times h\nu \sim 20 \text{ mW}$ if a fiber of $10 \mu\text{m}$ diameter and 0.5 m length, volume V is pumped with radiation at $1.48 \mu\text{m}$.

Figure 18.2 illustrates the principle of the erbium-doped fiber amplifier ($=\text{Er}^{3+}$; glass amplifier) as we will explain in the following sections. Pump radiation creates excited-impurity quasiparticles in a quasiband via optical transitions from a vacuum level to the upper part of the quasiband. Stimulated emission of radiation by transitions from the lower part of the quasiband to the vacuum level gives rise to amplification of radiation. The width ($\sim 50 \text{ meV}$) of the quasiband is small compared to the center energy (819 meV); the width of the quasiband depends on the type of glass and differs by a factor 2–3 for glasses of different composition. Pumping via higher levels has already been discussed (*see* Fig. 15.10a).

The erbium-doped fiber laser at room temperature is a quasiband laser (Sect. 4.3)—the intraband relaxation time (10^{-13} s) is much smaller than the relaxation time of energy levels with respect to relaxation to the ground state ($\tau_{\text{rel}}^* = 10^{-2} \text{ s}$). Intraband relaxation is a nonradiative relaxation. Population inversion occurs if the occupation number difference is larger than zero, $f_2 - f_1 > 0$. Because the halfwidth of the quasiband is comparable to kT , population inversion requires that about half of the erbium ions are in the excited state (Sect. 18.6).

18.2 Energy Levels of Erbium Ions in Glass and Quasiband Model

An energy level of a free Er^{3+} ion (Fig. 18.3) is characterized by the quantum number J of the total angular momentum; $J = 15/2$ in the ground state ($^4I_{15/2}$) and $J = 13/2$ in the first excited state ($^4I_{13/2}$). A crystalline electric field splits a level into a multiplet of $J + 1/2$ sublevels; because of Kramers degeneracy [121], a state with an odd J does not experience the complete lifting of the $2J + 1$ fold degeneracy. The splitting of the ground state level is larger than the splitting of the excited-state level as indicated in the figure for Er^{3+} ions in a LaF_3 crystal [146, 147].

In a glass, the Er^{3+} ions are randomly distributed on sites of different crystalline electric field. Boltzmann's statistics determines the occupancy of the sublevels of an ion; thermal equilibrium of the sublevel population of an ion is established via spin-lattice relaxation; at room temperature, nonradiative relaxation by spin-lattice relaxation processes lead to a fast establishment of thermal equilibrium in an erbium-doped glass as long as pump radiation is absent.

Multiplet splitting and crystal field variations suggest widths of energy distributions (~ 50 meV for the ground state levels and ~ 25 meV for the excited-state levels), which are of the order of kT at room temperature ($T =$ temperature; $k =$ Boltzmann's constant). In a laser medium consisting of a doped crystal, an excited ion loses its excitation energy mainly via a stimulated optical transition. But in a doped-glass medium, an ion excited via a pump process transfers its excitation to another ion, this again to another ion and so on. On average, a laser transition process occurs only after 10^{11} transfer processes.

As an example of a glass, we discuss a quartz glass ($=\text{SiO}_2$ glass). A two-dimensional structural model (Fig. 18.4) illustrates the structure of glass. The SiO_2 glass consists of silicon ion and oxygen ions. The silicon and oxygen ions do not form

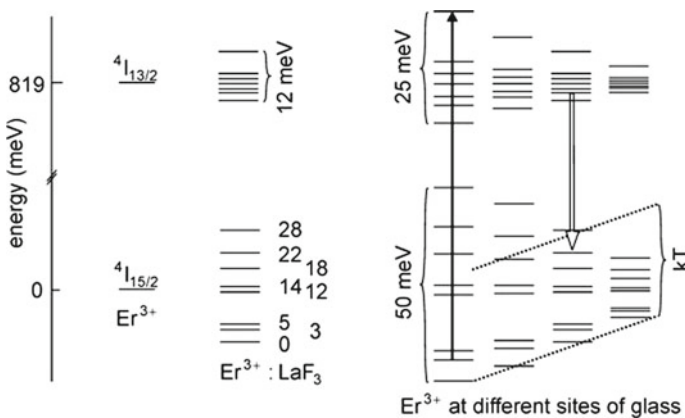


Fig. 18.3 Energy levels of free Er^{3+} ions, Er^{3+} ions in LaF_3 , Er^{3+} ions in a glass and a pump and a laser transition (arrows)

Fig. 18.4 Microscopic structure of glass

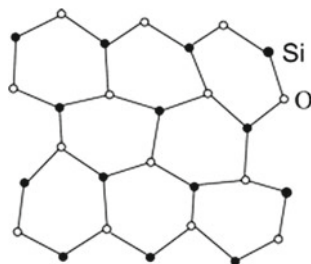
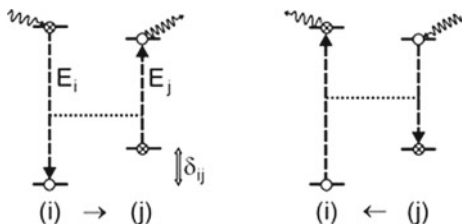


Fig. 18.5 A phonon-assisted energy transfer process and its reverse process



a periodic structure: the Si-O distance varies within the glass and the atomic arrangement shows no symmetry. Er^{3+} ions occupy different sites and therefore experience different crystal line fields. The energy of the ground state level, the energy of the excited state level, as well as the transition energy are different for erbium ions at different sites.

To discuss the role of energy transfer, we describe, for simplicity, an Er^{3+} ion as a two-level atomic system consisting of a ground state level and an excited-state level. An excited two-level system at site (i) with a transition energy E_i can transfer its excitation to a neighboring unexcited two-level system at site (j) that has a transition energy E_j (Fig. 18.5, left). The energies of the ground state levels differ by δ_{ij} . Energy conservation in a phonon assisted energy transfer process requires that

$$E_i + h\nu_{p1} = E_j + h\nu_{p2} + \delta_{ij}, \tag{18.2}$$

where ν_{p1} is the frequency of a phonon and ν_{p2} is the frequency of another phonon. The energy transfer rate depends on the concentration of impurity ions and the temperature of the glass. In the reverse process (Fig. 18.5, right), the sum of the energy of excitation of the ion at site (j), the energy of a phonon, and the energy of position is transferred to energy of excitation of ion (i) and of another phonon.

Energy transfer processes between rare earth ions in a glass at room temperature, with involvement of two phonons, first discussed in theoretical investigations [148, 149], are very efficient as experimental studies indicated [150, 151]. The microscopic process of energy transfer can be due to Coulomb interaction between two impurity ions.

Besides the two-phonon-assisted energy transfer, there are other energy transfer processes: resonant energy transfer (without the involvement of a phonon); energy

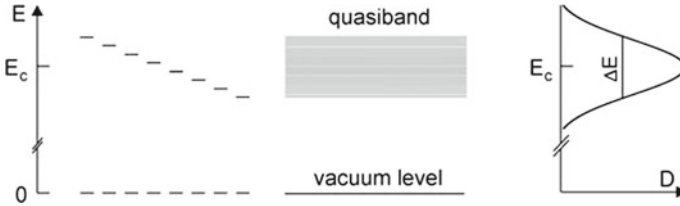


Fig. 18.6 Quasiband model of excited-impurity quasiparticles

transfer with involvement of one phonon; cross relaxation—an impurity ion in an upper level is excited to a higher level by transfer of energy from another ion that is in an excited state. The Förster mechanism (resonant energy transfer by dipole-dipole interaction) was first discussed in 1949 [152]. Some transfer processes are illustrated in Sect. 15.7.

A spectral hole burning study showed [153] that the broadening of an energy level of an excited Er^{3+} ion in a glass at room temperature corresponds to a lifetime of the order of 10^{-13} s (at a concentration of 1% Er_2O_3 by weight in glass). We associate the broadening to phonon-assisted energy transfer.

Now, we attribute the transition energies, sorted according to their values, to a quasiband (Fig. 18.6).

- $D(E)$ = density of states of the levels in the quasiband = number of levels per unit of volume and energy.
- $D(E)dE$ = number of levels within the energy interval $E, E + dE$ per unit of volume.
- N_0 = density of impurity ions = density of two-level atomic systems = number of impurity ions per unit of volume = number of lower levels per unit of volume (=number of upper levels per unit of volume).
- $N = N_2$ = density of excited ions.
- $N_0 - N$ = number of empty lower levels per unit of volume.
- N/N_0 = band filling factor.
- $f_2(E)$ = relative occupation number of level E = probability that the level with the energy E is occupied.
- $f_1 = 1 - f_2(E)$ = relative occupation number of the lower level = probability that the lower level, which belongs to the upper level of energy E , is occupied.
- $f_2 - f_1 = 2f(E) - 1$ = occupation number difference.
- $f_2(E)D(E)dE$ = density of occupied levels in the energy interval $E, E + dE$.

The integral over the density of states is equal to the density of impurity ions,

$$\int_0^\infty D(E)dE = N_0. \quad (18.3)$$

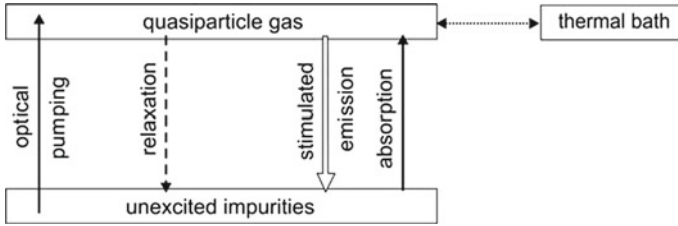


Fig. 18.7 Steady state of a gas of impurity-quasiparticles

We describe, for simplicity, the density of states by a Gaussian distribution,

$$D(E) = N_0 \times \sqrt{\frac{4 \ln 2}{\pi}} \frac{1}{\Delta E} \exp \left[-\frac{\ln 2 \times (E - E_c)^2}{\Delta E^2/4} \right]. \quad (18.4)$$

E_c is the center and ΔE the halfwidth of the distribution.

Because of the phonon-assisted energy transfer processes, the quasiparticles interact with each other and couple to the thermal bath. The coupling to the thermal bath gives rise to the formation of a thermal equilibrium of the population in the quasiband (Fig. 18.7). At steady state, the average number of quasiparticles is constant. Continuous optical pumping compensates the loss of quasiparticles that is due to relaxation (mainly caused by spontaneous emission of radiation) and due to the net effect of stimulated emission and absorption of radiation.

Our model does not take into account that the ground state as well as the excited state of a single Er^{3+} ion are multiplets (due to crystal field splitting). Without pumping, the population in a multiplet of the ground state is in thermal equilibrium. This equilibrium is established via spin-lattice relaxation processes. During optical pumping, the ensemble of occupied ground state levels is not in a thermal equilibrium.

18.3 Quasi-Fermi Energy of a Gas of Excited-Impurity Quasiparticles

An energy level of the quasiband is, according to the Pauli principle, either empty or occupied with one quasiparticle. We apply to the ensemble of quasiparticles Fermi's statistics and describe the average occupation number of an energy level by the Fermi–Dirac distribution function

$$f_2(E) = \frac{1}{\exp[(E - E_F)/kT] + 1}. \quad (18.5)$$

E_F is the quasi-Fermi energy of the quasiparticle gas and T the temperature of the glass. The quasi-Fermi energy follows from the condition that

$$\int_0^{\infty} f_2(E)D(E)dE = N. \quad (18.6)$$

N is the density of quasiparticles. The probability to find a quasiparticle in a level of energy E is $f_2(E)$. The probability that the ground state level, which corresponds to the excited-state level of energy E , is occupied, is $f_1 = 1 - f_2$.

We introduce dimensionless variables $x = E/kT$, $a = E_F/kT$, $b = E_c/kT$, $w = \Delta E/kT$ and write (assuming a Gaussian distribution of the density of states) the condition (18.6) in the form

$$\int_0^{\infty} \frac{\exp[-4 \ln 2(x - b)^2/w^2] dx}{\exp(x - a) + 1} = 1.06 w \frac{N}{N_0}. \quad (18.7)$$

If $b \gg 1$ ($E_c \gg kT$), which is the case for glass amplifiers and lasers, a numerical analysis of (18.7) yields a quasi-Fermi energy that does not depend on w ; the integral is finite only in a small range of x around b and zero otherwise. The quasi-Fermi energy E_F (Fig. 18.8) increases with increasing filling factor N/N_0 and is equal to E_c at half filling; E_F is $-\infty$ at zero quasiband filling ($N = 0$) and $+\infty$ at complete filling ($N = N_0$). The quasi-Fermi energy E_F depends linearly on N/N_0 in a large range of the filling factor,

$$E_F = E_c + 4.44 \times (N/N_0 - 0.5) kT. \quad (18.8)$$

Figure 18.9 shows the occupation number difference $f_2 - f_1$ for quasiparticles at the center of the quasiband ($E = E_c$). The occupation number difference is -1 for $N = 0$. With increasing N , $f_2 - f_1$ increases, becomes zero at half filling of the quasiband and increases further. At complete filling ($N = N_0$), the occupation number difference is unity. The occupation number difference shows a linear dependence on the filling factor,

$$f_2 - f_1 \approx 2.22 (N/N_0 - 1/2), \quad (18.9)$$

with small deviations near $N/N_0 = 0$ and $N/N_0 = 1$.

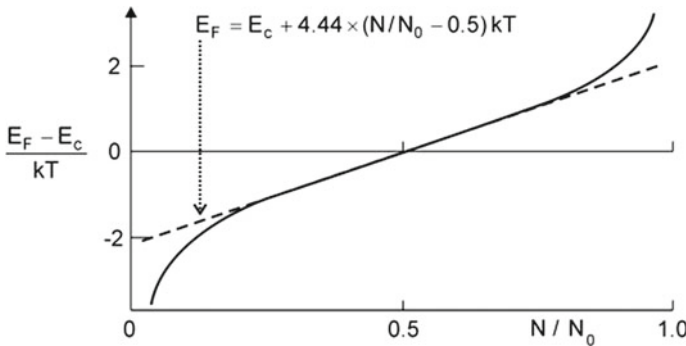


Fig. 18.8 Dependence of the quasi-Fermi energy on the filling factor of a quasiband

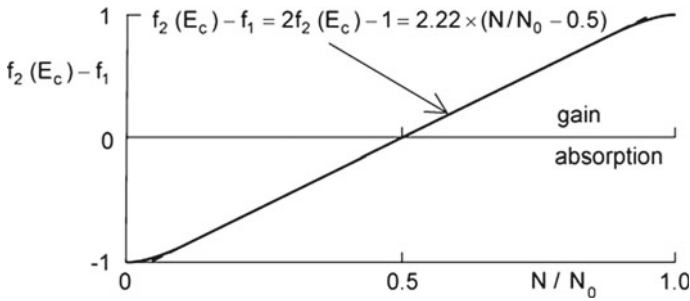


Fig. 18.9 Occupation number difference for quasiparticles in the center of the quasiband

At the center of the quasiband, the occupation number difference (see Fig. 18.9) increases linearly over almost the whole range of the filling factor,

$$f_2(E_c) - f_1 = 2f_2(E_c) - 1 = 2.22 \times (N/N_0 - 0.5). \quad (18.10)$$

The linear dependence of the occupation number difference on the filling factor, for $E = E_c$, appears to be characteristic for a Gaussian shape of the density of states of the quasiband; there are only small deviations from the linear dependence, occurring at N/N_0 near 0 and 1. The linear slope is slightly (11%) larger than for an ensemble of two-level systems that all have the same transition energy. We will show that $f_2 - f_1 \geq 0$ corresponds to gain and $f_2 - f_1 \leq 0$ to absorption.

A Fourier expansion of $f_2(E)$ around E_c indicates that the linear dependence of the occupation number difference $f_2(E_c) - f_1$ on N/N_0 follows directly from the linear dependence of the quasi-Fermi energy E_F on N/N_0 (Problem 18.3). The linear dependence of $f_2(E_c) - f_1$ extends, however, over a much larger range of the filling factor than the linear dependence of the quasi-Fermi energy.

18.4 Condition of Gain of Light Propagating in a Fiber

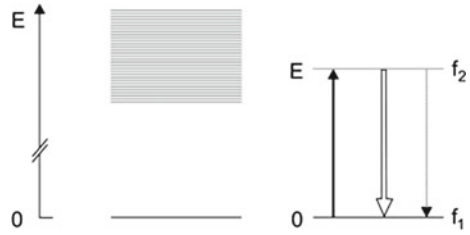
Electromagnetic radiation (frequency ν) that has a continuous energy distribution around the photon energy $h\nu = E$ interacts with a quasiparticle in a level of energy E (Fig. 18.10) by absorption, stimulated and spontaneous emission. The transition rate (=number of transitions per s and m^3) of stimulated emission is given by

$$r_{em}(h\nu) = \bar{B}_{21} f_2 \rho(h\nu) \quad (18.11)$$

and the rate of absorption by

$$r_{abs}(\nu) = r_{abs}(h\nu) = \bar{B}_{12} f_1 \rho(h\nu). \quad (18.12)$$

Fig. 18.10 Radiative transitions between an energy level of a quasiband and the vacuum level



We use the quantities:

- E = transition energy.
- \bar{B}_{21} = Einstein coefficient of stimulated emission (in units of $\text{m}^3 \text{s}^{-1}$); $\bar{B}_{21} = h B_{21}$ (Sect. 6.6).
- \bar{B}_{12} = Einstein coefficient of absorption; $\bar{B}_{12} = \bar{B}_{21}$.
- f_2 = probability that the upper level is occupied.
- $f_1 = 1 - f_2$ probability that the lower level is occupied.
- $\rho(h\nu)$ = spectral energy density of the radiation on the energy scale.

It is convenient to express the energy density on the energy scale.

The difference between the rates of stimulated emission and absorption is

$$r(h\nu) = \bar{B}_{21}(f_2 - f_1)\rho(h\nu). \quad (18.13)$$

Stimulated emission prevails if $f_2 - f_1 > 0$ or $f_2 > 1/2$. This is the condition for gain of light propagating in a fiber. The spontaneous emission rate is

$$r_{\text{sp}} = A_{21}f_2. \quad (18.14)$$

A_{21} is the Einstein coefficient of spontaneous emission.

18.5 Energy Level Broadening

The phonon-assisted energy transfer processes cause a broadening of the levels of the quasiband (Fig. 18.11). We describe the broadening of a level of energy E by a lineshape function $g(h\nu - E)$ that has a halfwidth δE and is normalized,

$$\int g(h\nu - E) d(h\nu) = 1. \quad (18.15)$$

The integral over all contributions $g(h\nu - E)d(h\nu)$ in the photon energy interval $h\nu$, $h\nu + d(h\nu)$ is unity. The net transition rate of monochromatic radiation, i.e., of radiation with $\rho(h\nu) \neq 0$ in the energy interval $h\nu$, $h\nu + d(h\nu)$, where $d(h\nu) \ll \delta E$, is given by

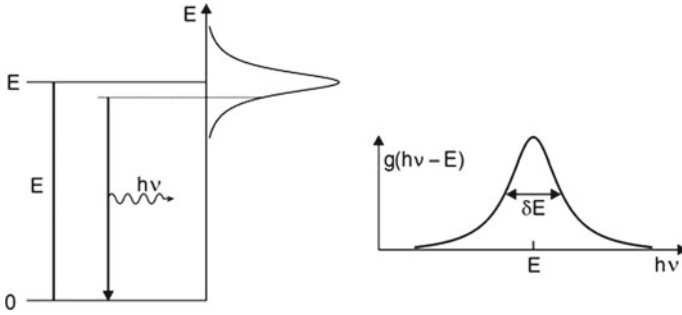


Fig. 18.11 Energy level broadening

$$(r_{\text{em}} - r_{\text{abs}})_{h\nu} d(h\nu) = \bar{B}_{21} g(h\nu - E)(f_2 - f_1) \rho(h\nu) d(h\nu). \quad (18.16)$$

Supposing that the lineshape function is a Lorentzian, we can write

$$g(h\nu - E) = \frac{\delta E}{2\pi} \frac{1}{(h\nu - E)^2 + (\delta E/2)^2}, \quad (18.17)$$

where δE is the halfwidth of the level broadening. The net transition rate is

$$r(\nu) = r(h\nu) = r_{\text{em}} - r_{\text{abs}} = \int \bar{B}_{21} g(h\nu - E)(f_2 - f_1) \rho(h\nu) d(h\nu). \quad (18.18)$$

Introducing the energy density $u = \int \rho(h\nu) d(h\nu) = Zh\nu$, where Z is the density of photons, leads to the net transition rate

$$r(\nu) = h\nu \bar{B}_{21} g(h\nu - E)(f_2 - f_1) Z. \quad (18.19)$$

The net transition rate is proportional to the occupation number difference $f_2 - f_1 = 2f_2 - 1$ and to the photon density Z . The condition of gain is the same as derived for the case of neglected energy level broadening,

$$f_2 - f_1 = 2f_2(E) - 1 > 0 \quad \text{or} \quad f_2(E) > 1/2; \quad (18.20)$$

gain occurs for radiation of quantum energies

$$h\nu < E_F. \quad (18.21)$$

Optical pumping is possible by using radiation of a quantum energy $h\nu$ that is larger than the quasi-Fermi energy E_F . The mechanism leading to the quasi-Fermi distribution is the intraband relaxation. Due to phonon-assisted energy transfer, the excited two-level atomic systems lose a portion of their excitation energy to phonons. This leads, at room temperature, to the formation of the quasi-Fermi distribution in

the quasiband. After the formation of a quasithermal equilibrium, the excited two-level atomic systems still interact with phonons. Accordingly, each upper level is energetically broadened due to energy transfer processes. The width of a broadened energy level is $\delta E \approx \hbar/\tau_{\text{in}}$, where τ_{in} is the scattering time, i.e., the time between two energy transfer events. The scattering time τ_{in} depends on temperature. At room temperature, the occupation number of thermal phonons is large at phonon energies $kT \sim 25$ meV. Thus, a few energy transfer events (per excited two-level system) establish a quasiequilibrium after a few scattering events. Therefore, we regard τ_{in} as the intraband relaxation time.

The intraband relaxation time ($\sim 10^{-13}$ s) of Er^{3+} :glass at room temperature is much shorter than the lifetime (of the order of 10 ms) of an upper level with respect to spontaneous emission of a photon. The width of the broadening of an upper level, $\hbar/\tau_{\text{in}} \sim 4$ meV, is small compared to the range ($\sim kT$) of populated levels.

18.6 Calculation of the Gain Coefficient of a Doped Fiber

The temporal change of the density of excited ions due to stimulated transitions is

$$\frac{dN}{dt} = -h\nu \int \bar{B}_{21} g(h\nu - E)(f_2 - f_1) D(E) dE \times Z, \quad (18.22)$$

It follows that the temporal change of the photon density Z is given by the relation

$$dZ/dt = -dN/dt = \gamma Z, \quad (18.23)$$

where

$$\gamma = h\nu \int \bar{B}_{21} D(E)(f_2 - f_1) g(h\nu - E) dE \quad (18.24)$$

is the growth coefficient of radiation of frequency ν . With $dt = ndz/c$, where z is the direction of propagation of the radiation (along the fiber axis), c is the speed of light in vacuum, n (~ 1.5) the refractive index of the fiber glass, we find

$$dZ/dz = \alpha Z, \quad (18.25)$$

where

$$\alpha = \frac{n}{c} h\nu \int \bar{B}_{21} D(E)(f_2 - f_1) g(h\nu - E) dE \quad (18.26)$$

is the gain coefficient. The level broadening due to energy transfer is small compared to kT . Therefore, we can replace $g(h\nu - E)$ by a delta-function, $\delta(h\nu - E)$, and find

$$\alpha(\nu) = (n/c) h\nu \bar{B}_{21} D(E)(f_2 - f_1), \quad (18.27)$$

where $(f_2 - f_1) = 2f_2(E) - 1$ and $E = h\nu$.

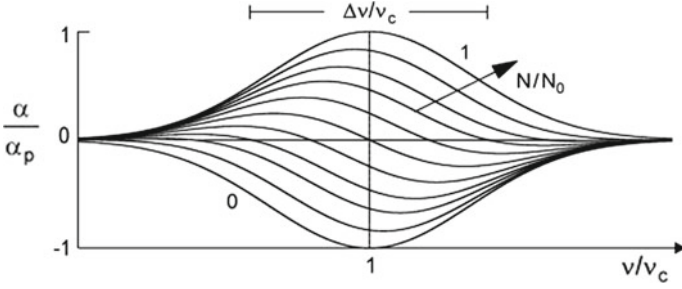


Fig. 18.12 Gain coefficient at different band filling factors N/N_0 (in steps of 0.1)

Under the assumption that B_{21} is the same for all two-level systems and does therefore not depend on E , the peak gain coefficient is

$$\alpha_p = (n/c)h\nu_c \bar{B}_{21} D(E_c). \quad (18.28)$$

Then the slope of the gain coefficient curves is given by the simple expression

$$\alpha(\nu)/\alpha_p = f_2 - f_1 = 2f_2(E) - 1; \quad E = h\nu. \quad (18.29)$$

Gain coefficient curves (Fig. 18.12) show that the range of gain increases with increasing quasiband filling according to the increase of the frequency

$$\nu_F = E_F/h. \quad (18.30)$$

The frequency ν_F is a *transparency frequency*. At complete filling, the gain coefficient has the same slope as the density of states and reaches the peak gain coefficient α_p at the center frequency $\nu_c = E_c/h$. If the quasiband is empty, the absorption coefficient has the same profile as the density of states.

From the peak gain coefficient, we obtain a peak gain cross section according to the relation

$$\alpha_p = N_0 \sigma_p. \quad (18.31)$$

We find

$$\sigma_p = \frac{n}{c} h\nu \bar{B}_{21} D(E_c)/N_0 = 1.48 \frac{\Delta\nu_{\text{hom}}}{\Delta\nu} \frac{(\lambda/n)^2}{2\pi}, \quad (18.32)$$

with the quantities: $\Delta\nu = \Delta E/h$; $A_{21} = 8\pi\nu^3(n/c)^{-3} \bar{B}_{21}$ = Einstein coefficient of spontaneous emission; $\lambda = c/\nu_c$. Thus, σ_p has the same value as the peak gain cross section of an ensemble of noninteracting two-level systems with transitions of Gaussian shape.

The condition of gain

$$(f_2 - f_1) = 2f_2(E) - 1 \geq 0 \quad \text{with} \quad E = h\nu \quad (18.33)$$

means that gain occurs at frequencies

$$\nu < \nu_F(N/N_0) = E_F(N/N_0)/h \quad (18.34)$$

and that $\alpha(\nu_F) = 0$. It follows that the transparency density N_{tr} is, in a large range of the filling factor, given by

$$\frac{N_{tr}}{N_0} = 0.5 + \frac{E_F - E_c}{4.44 kT} = 0.5 + \frac{\nu_F - \nu_c}{4.44 kT/h}. \quad (18.35)$$

Example Gain coefficient of a fiber doped with 1% Er_2O_3 by weight ($N_0 = 7 \times 10^{25} \text{ m}^{-3}$) at a filling factor $N/N_0 = 0.6$ (see Fig. 18.1).

- $A_{21} = 100 \text{ s}^{-1}$; $\Delta\nu_{\text{hom}} = A_{21}/(2\pi) \sim 16 \text{ s}^{-1}$.
- $\bar{B}_{21} = 4.0 \times 10^{-18} \text{ m}^3 \text{ s}^{-1}$.
- $E_c = 819 \text{ meV}$; $\nu_c \sim 198 \text{ THz}$.
- $c/n = 2 \times 10^8 \text{ m s}^{-1}$.
- $\Delta E = 50 \text{ meV} = 8 \times 10^{-21} \text{ J}$; $\Delta\nu \sim 12 \text{ THz}$.
- $D(E_c) = 8.3 \times 10^{45} \text{ m}^{-3} \text{ J}^{-1}$.
- $\alpha_p = 22 \text{ m}^{-1}$; $\sigma_p = 3.2 \times 10^{-25} \text{ m}^2$.

The gain coefficient (at a filling factor of 0.6) is positive below a frequency that is slightly larger than ν_c while a range of absorption follows at higher frequency; the maximum gain coefficient ($\sim 9 \text{ m}^{-1}$) is slightly smaller than half the peak gain coefficient α_p .

Figure 18.13 illustrates our result. Gain occurs up to the transparency frequency $\nu_F = E_F/h$. The quasi-Fermi energy E_F and thus ν_F increase with increasing band filling.

According to the linear dependence of the occupation number difference at the center of the quasiband on the filling factor (see Fig. 18.9), we find

$$\alpha(\nu_c)/\alpha_p \approx 2.22 (N/N_0 - 1/2); \quad (18.36)$$

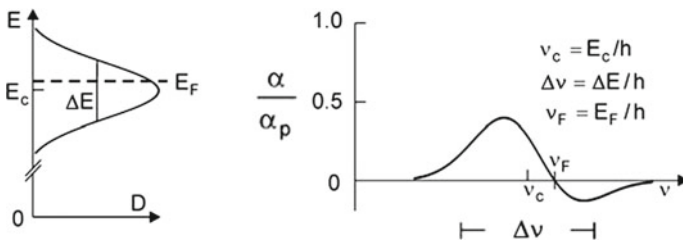
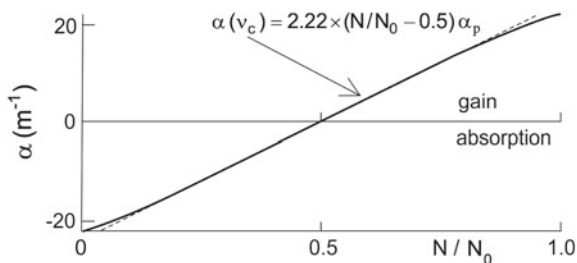


Fig. 18.13 Quasi-Fermi energy and transparency frequency

Fig. 18.14 Gain coefficient of an erbium-doped fiber at the center frequency
 $\nu_c = E_c/h$; $\alpha_p = N_0 \sigma_p$,
 $N_0 = 7 \times 10^{25} \text{ m}^{-3}$, and σ_p
 $= 3.2 \times 10^{-25} \text{ m}^2$



the gain coefficient at the frequency $\nu_c = E_c/h$ increases linearly with the filling factor (Fig. 18.14).

18.7 Different Effective Gain Cross Sections

Here, we introduce three different effective gain cross sections: effective gain cross section σ ; effective gain cross section $\bar{\sigma}_{\text{eff}}$; effective gain cross section σ_{eff} .

Figure 18.15 shows gain coefficients (solid lines) at different quasiband filling factors. The maximum gain coefficient α_{max} (dashed) depends on the filling factor. We can relate the maximum gain coefficient and the density of quasiparticles (i.e., the density of excited ions),

$$\alpha_{\text{max}} = N \sigma; \tag{18.37}$$

the effective gain cross section σ (Fig. 18.6, dashed) increases with increasing filling factor, from zero for the empty quasiband to σ_p at complete quasiband filling.

The effective gain cross section

$$\bar{\sigma}_{\text{eff}} = (d\alpha_{\text{max}}/dN)_{N/N_0} \tag{18.38}$$

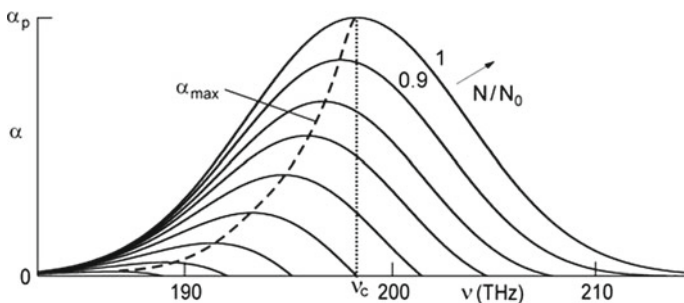
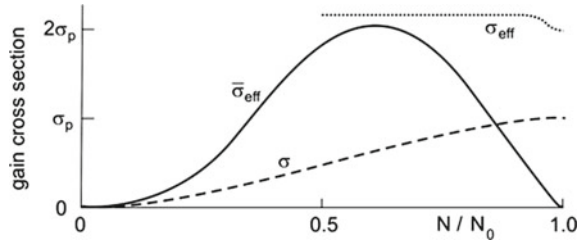


Fig. 18.15 Gain coefficient at different filling factors

Fig. 18.16 Effective gain cross sections of Er^{3+} in an erbium-doped fiber



describes the change of α_{\max} with N . With increasing N/N_0 , the effective gain cross section $\bar{\sigma}_{\text{eff}}$ (Fig. 18.16, solid line) increases from zero near $N/N_0 = 0$, shows a maximum ($\sim 2\sigma_p$) for $N/N_0 \sim 0.6$, then decreases and approaches zero near $N/N_0 = 1$.

We can introduce another effective gain cross section, σ_{eff} , writing

$$\alpha(\nu_c) \approx 2.22(N/N_0 - 1/2)(n/c)h\nu\bar{B}_{21}D(E_c) = (N - N_0/2)\sigma_{\text{eff}} \quad (18.39)$$

and find

$$\sigma_{\text{eff}} \approx 2.22(n/c)h\nu\bar{B}_{21}D(E_c) = 2.22\sigma_p. \quad (18.40)$$

The effective gain cross section σ_{eff} (Fig. 18.16, dotted) has a constant value ($2.22\sigma_p$) over a large range of the filling factor, from $N/N_0 = 0.5$ to nearly $N/N_0 = 1$, where it decreases to $2\sigma_p$. At complete filling, $\sigma_{\text{eff}} = 2\sigma_p$; the factor 2 is due to the different reference values, $N/N_0 - 0.5$ and N , respectively. At smaller band filling, σ_{eff} exceeds $2\sigma_p$ because band filling in the center of the quasiband leads to stronger gain than filling in the wing of the band for $N/N_0 \rightarrow 1$.

The effective gain cross section

$$\sigma_{\text{eff}} = (d\alpha/dN) \quad (18.41)$$

describes, for radiation of frequency ν_c , the gain cross section related to the two-level systems that are excited above half filling; $N_0/2$ is the transparency density for radiation of frequency ν_c .

Here, we can ask: does the gain coefficient curve show a narrowing near complete quasiband filling, i.e., when almost all erbium ions (for instance 90%) are in the excited state? In this case, the energy transfer processes strongly slow, particularly in the wings of the quasiband.

18.8 Absorption and Fluorescence Spectra of an Erbium-Doped Fiber

The shape of an absorption curve is given by

$$\bar{\alpha}_{\text{abs}} = \alpha_{\text{abs}}(\nu)/\alpha_p = f_1 - f_2 = 1 - 2f_2(E), \tag{18.42}$$

where $E = h\nu$ and where α_p is the absorption coefficient at the frequency ν_c at zero quasiband filling. The shape of a fluorescence curve is given by

$$\bar{S}_\nu(\nu) = S_\nu(\nu)/S_{\nu,p} = f_2(E); \quad E = h\nu. \tag{18.43}$$

$S_\nu(\nu)$ is the spectral distribution of the fluorescence radiation. $S_{\nu,p}$ is the peak intensity, namely the intensity at the frequency ν_c in the case of complete quasiband filling. We neglect the frequency dependence of the Einstein coefficient of spontaneous emission.

Figure 18.17 shows an absorption curve and a fluorescence curve both for weak quasiband filling ($N/N_0 = 0.1$). The absorption curve is slightly blue-shifted with respect to the absorption curve for zero quasiband filling. The fluorescence curve is red-shifted. The absorption and the fluorescence curves have different shapes. The shapes of the curves as well as the frequencies of their maxima depend on the filling factor.

The filling factor relates the absorption coefficient and the shape of the fluorescence curves according to the expression

$$\bar{S} = \frac{f_2}{1 - 2f_2} \times \bar{\alpha}_{\text{abs}}. \tag{18.44}$$

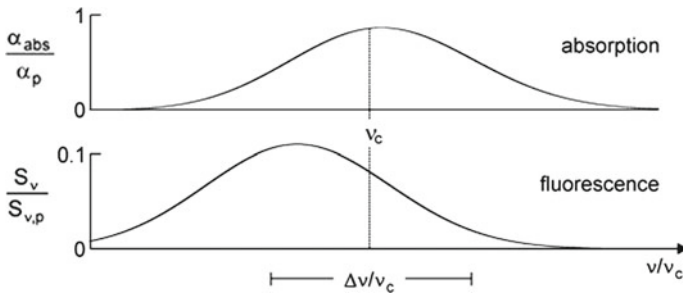


Fig. 18.17 Shapes of an absorption and a fluorescence curve of a fiber medium at the filling factor $N/N_0 = 0.1$

At weak quasiband filling ($N/N_0 \ll 1$), the relation is

$$\bar{S} = f_2 \times \bar{\alpha}_{\text{abs}} = \frac{1}{\exp[(E - E_F)/kT] + 1} \times \bar{\alpha}_{\text{abs}}. \quad (18.45)$$

In this case, the shape of the fluorescence curve is determined by the product of the Fermi–Dirac distribution function and the absorption coefficient.

It is possible to modify the quasiparticle model taking into account that B_{21} can have different values for ions at different sites in a glass and that the density of states does not have a Gaussian shape. An analysis of absorption and fluorescence spectra measured for different filling factors N/N_0 (and different sample temperatures) may provide detailed information on $B_{21}(v)$ and $D(v)$.

There remains the question how to take account of the multiplet splitting, especially of the occupied sublevels of the ground state. During optical pumping, the population of the ensemble of sublevels of the nonexcited ions is not in thermal equilibrium as already mentioned.

18.9 Experimental Studies and Models of Doped Fiber Media

The gain coefficient curves at different filling factors (*see* Fig. 18.12) and the absolute values of the gain coefficients (*see* Fig. 18.1) are, in principle, in accord with experimental results. However, experimental studies of the shape of absorption curves, gain curves, and fluorescence curves of erbium-doped fibers indicate the following:

- The profiles of absorption spectra and of fluorescence spectra are non-Gaussian [154]; this shows that the densities of states of quasiparticles have non-Gaussian profiles and that—most likely— B_{21} does not have a constant value.
- The profiles depend on the composition of a fiber glass; fibers can consist of various types of glasses (silicate, phosphate, germanite, fluorite, fluorozirconate glass).
- The fluorescence spectrum is red-shifted relative to the absorption spectrum—in accord with the results (*see* Fig. 18.17) obtained with the quasiparticle model.

We mention two other models that are mostly used to describe fluorescence, absorption, and gain curves of fiber media:

- Three-level laser model (Fig. 18.18a). It describes gain and absorption of an erbium-doped fiber amplifier [155, 156]; numerical simulations provide gain coefficient curves that show a similar behavior as the gain curves (Fig. 18.12) obtained by the analytical expression (18.29).
- Three-level laser medium of the ruby laser type (Fig. 18.18b). It describes amplifiers and lasers, which are strongly pumped via high-lying pump levels [157, 158].

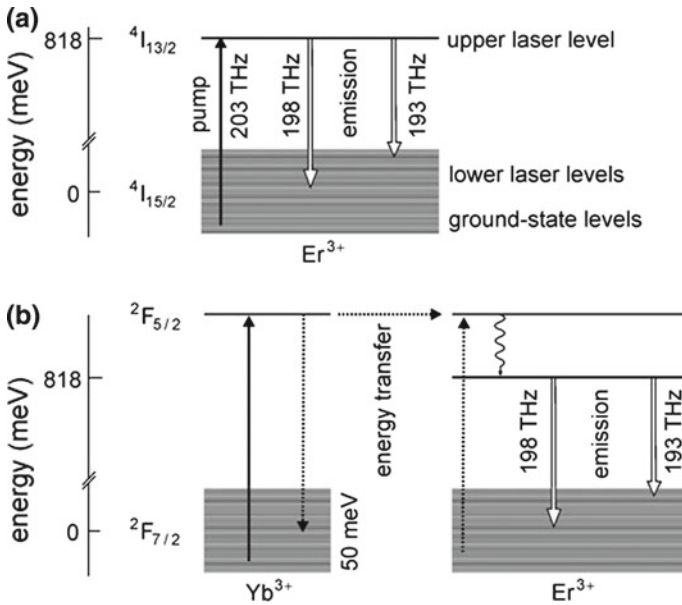


Fig. 18.18 Models of fiber amplifiers and lasers. **a** Three-level laser model of the erbium-doped fiber amplifier. **b** Ruby laser type model of an erbium-doped fiber laser

These models assume a quasithermal equilibrium of the population of the ground state levels. Although the assumption is not fully justified, the models provide a basis of the description of optical properties of a fiber.

The quasiband model should also be applicable to analyze active media of fiber lasers and amplifiers strongly pumped via high-lying energy levels mentioned in Sect. 15.7:

- 1.05- μm ytterbium-doped fiber laser [159].
- 1.5- μm ytterbium/erbium-doped fiber amplifiers [160].
- Thulium-doped fiber laser [161, 162].
- 2.1- μm holmium-doped fiber laser [163].
- 3- μm ytterbium/erbium-doped fiber laser [164, 165].

The quasiparticle model predicts a narrowing of the gain curve at nearly complete population inversion. When nearly all impurity ions are in the excited state, the rate of phonon-assisted energy transfer processes slows down; at complete population inversion, energy transfer processes are no longer possible.

References [140–165].

Problems

18.1 Fiber laser. Estimate the efficiency of an erbium-doped fiber laser pumped with a pump power twice the threshold pump power if the laser is pumped with 1480-nm radiation or if it is pumped with 980-nm radiation.

18.2 A glass contains erbium ions of a density $N_0 = 7 \times 10^{25} \text{ m}^{-3}$.

- Determine the average distance r_0 between neighboring erbium ions.
- Estimate the number of neighbors of an erbium ion that lie in spherical shells (thickness r_0) with the radii r_0 and $2r_0$; $2r_0$ and $3r_0$; $3r_0$ and $4r_0$; furthermore with the radii sr_0 and $sr_0 + r_0$ with $s \gg 1$.

18.3 Occupation number difference in an erbium-doped fiber amplifier.

- Show that the occupation number difference at the energy E_c for Fermi energies in the vicinity of E_c is given by $f_2 - f_1 = 2f(E_c) - 1 \approx (E_F - E_c)/2kT$.
- How large is $f_2 - f_1$ if $E_F = E_c + kT$?
- Determine the percentage of energy levels of the quasiband lying in the energy range $E_c - \Delta E/2$, $E_c + \Delta E/2$.

18.4 Discuss why the following lasers do not belong to the type “quasiband laser”:

- Titanium–sapphire laser, alexandrite laser; and, generally, vibronic lasers.
- Helium–neon laser.
- Continuous wave CO_2 laser and TEA CO_2 .

18.5 Density of states. We consider the following case: the density of states of quasiparticles in an erbium-doped fiber is the sum of two densities of state, $D = D_1 + D_2$; the center frequencies have a frequency distance of $4kT$ ($T = 300 \text{ K}$); the halfwidth of both densities of states is $2kT$.

- Estimate the maximum gain coefficient α_{max} .
- Estimate the maximum gain coefficient in the case that the center frequencies have a frequency distance of kT .

18.6 Present arguments that show that it is most likely that the spontaneous lifetime τ_{sp} of the ${}^4\text{I}_{13/2}$ level of erbium ions in a glass fiber depend on the quasiband filling factor.

18.7 Einstein coefficients. Consider an impurity-doped fiber with a Gaussian shape of the density of states of quasiparticles.

- Design a dependence $B_{21}(E)$ that leads to a double peak in the gain curve.
- Then discuss the dependence of τ_{sp} on the filling factor.

18.8 Temperature coefficient. Make use of the quasiparticle model to estimate the temperature coefficient (in units of $\text{dB}/^\circ\text{C}$) of an erbium-doped fiber amplifier of 10 m length for the temperature ranges 10–20, –50 to –40 and 50–60 $^\circ\text{C}$:

- (a) If the frequency of the radiation is equal to the center frequency.
- (b) If the frequency of maximum gain occurs at a filling factor of 0.6.

18.9 Fiber laser and fiber amplifier. Determine the gain of radiation passing through an erbium-doped fiber (length 16 m) pumped at twice the transparency density; for data, see Sect. 18.6.

18.10 Why is the population of the multiplet levels of the ground state of Er^{3+} not in thermal equilibrium during optical pumping?

18.11 Spectral diffusion and quasiband model.

Describe diffusion of excitation energy in an infinitely long rectangular slab of a glass containing a large concentration of Er^{3+} ions. At time $t = 0$, excitation energy E_c at the center of the Gaussian quasiband is homogeneously deposited over the slab, with the quasiparticle density N_0 . [*Hint*: apply the one-dimensional diffusion equation $\partial f / \partial t = D_E \partial^2 f / \partial E^2$, where $f(E - E_c, t)$ is the distribution function and D_E the spectral diffusion constant, and replace the Gaussian shape of the density of states by a constant.]

- (a) Show that $f(E - E_c, t) = N_0 / (2\sqrt{2D_E t}) \exp(-(E - E_c)^2 / 4D_E t)$.
- (b) Determine the variance and the halfwidth (FWHM) of the distribution at time t .
- (c) Determine the average frequency range over which excitation energy of a two-level system traveled in a random walk after $z (\gg 1)$ inelastic scattering processes.
- (d) Estimate the spectral diffusion constant, assuming that the average energy transferred in a spectral diffusion process according to (18.2) is $\delta = 0.1$ meV. [*Hint*: the spectral diffusion constant is $D_E = (1/3) v_E^2 / \tau$, where $v_E = \delta / \tau$ is the velocity in the energy space and $\tau (\approx 10^{-13} \text{ s})$ the lifetime of an excited state level with respect to an energy transfer process.]
- (e) How many scattering events are necessary to distribute the energy over the whole width of a quasiband of a width of 50 meV? Show that the corresponding time is still much shorter than the spontaneous lifetime of an excited state. (This is an essential condition for the applicability of the quasiband model.) [*Hint*: neglect the influence of thermal effects.]
- (f) Determine, for the given numbers, the value of the maximum of the distribution function for the case that the energy is distributed over the whole quasiband.

18.12 Range of validity of the quasiband model.

The quasiband model is applicable for glass laser materials at room temperature. Cooling of the material leads to a slowing down of the energy transfer processes. Determine the temperature at which the quasiband model is no longer applicable if the lifetime of an excited state level with respect to an energy transfer process is inversely proportional to temperature. [*Hint*: make use of data of the preceding problem.]

18.13 Spectral-spatial diffusion in an active glass medium.

In a fiber laser, the laser field as well as the pump field is non-uniform over the cross section. Redistribution occurs by both spatial and spectral diffusion. It is the purpose of this problem to study the speed of redistribution by spectral-spatial diffusion.

- (a) Describe spectral-spatial diffusion by a one-dimensional differential equation for the distribution $f(x, E, t)$.
- (b) Solve the equation for the following case: The fiber has a quadratic cross section. At time $t = 0$, excitation energy is deposited at the center of a Gaussian quasi-band with a homogenous distribution over the cross section at $x = 0$. The two-dimensional quasiparticle density for $t = 0$ and $x = 0$ is N_0 ; x is the direction of the fiber.

18.14 Spectral-spatial diffusion in an erbium-doped glass fiber laser.

Apply the results of the preceding problem to a cw erbium-doped fiber laser assuming that the pump radiation is homogeneously distributed in the fiber. Assume that the laser field has a nearly Gaussian distribution within the fiber.

- (a) How broad is the spatial hole?
- (b) Estimate the time it takes to fill the spatial hole.
- (c) Estimate the time it takes to fill the spectral hole.
- (d) How deep is the spectral hole?

18.15 Formulate the formulas describing spectral-spatial diffusion (a) in dimensionless units and (b) in the frequency space $\nu = E/h$ instead of the energy space.